ELSEVIER

Coordination Chemistry Reviews
175 (1998) 43–58

COORDINATION CHEMISTRY REVIEWS

Substituent effects in dinuclear paddlewheel compounds: electrochemical and spectroscopic investigations☆

Tong Ren *

Department of Chemistry, Florida Institute of Technology, Melbourne, FL 32901, USA

Received 30 January 1998; accepted 24 March 1998

Contents

Abstract

This review summarizes substituent effects in dinuclear compounds supported by diarylformamidinate (form) ligands, where aryl is phenyl substituted with various polar groups (X). These dinuclear compounds, $M_2(\text{form})_4(L_{ax})_m$ with M as Mo, Ru, Rh, or Ni, L_{ax} as either neutral or anionic axial ligand, and $m = 0$–2, may undergo up to three (quasi)reversible

---

☆ Dedicated to Professor F. Albert Cotton on the occasion of his reception of the Prestley Medal.

* Present address: Department of Chemistry, University of Miami, Coral Gables, FL 33124-0431, USA. E-mail: tren@umiami.ir.miami-edu.

PII: S0010-8545(98)00202-1

one-electron, metal-centered redox processes. Linear correlations have been established between the electrode potentials ($E_{1/2}$, E_{pc} or E_{pa}) and the substituent constants (σ) according to the following Hammett equation: $\Delta E = E(X) - E(H) = \rho(\Sigma \sigma)$, with the reaction constant ρ ranging from + 60 to + 100 mV. The existence of such relationships indicates that the energy levels of the frontier orbitals of dinuclear species are controlled precisely by the substituent within each series, and generally decrease with an increase in the electron withdrawing ability of the substituent. However, nearly identical UV–vis absorption spectra were observed within each homologous series, and one can infer a minimal substituent perturbation on the distribution of upper valence molecular orbitals. Axial ligation of organic π acids such as CO and phenylacetylide in both the diruthenium and dirhodium series also provides insight to the activation of these substrates by the dinuclear core, and the linear free energy relationship therein. A brief overview of other investigations of substituent effects in dinuclear compounds is provided also.

Keywords: Substituent effects; LFER; Dinuclear compounds; Formamidinate

1. Introduction

The substituent effect in coordination chemistry is a relatively young field, in comparison with the much developed organic counter-part [1–4]. One well-investigated system is the metal complexes of *meso*-tetraphenylporphyrin, where redox tuning through substitution both on the phenyl rings and at the β positions of the pyrrole rings have been extensively examined in many laboratories [5]. In particular, perhalogenation at the periphery of metallo-tetraphenylporphyrins has led to significant anodic shifts in the electrode potentials for the redox couples localized at both the porphyrin ring and the metal center. As catalytic mimics of *Cyt.* P_{450} and other oxidases/oxygenases, these polyhalometalloporphyrins are robust towards oxidative degradation and exhibit much enhanced electrophilicity towards hydrocarbon substrates [6,7]. Substituents also influence the reactivity of mononuclear compounds in thioether formation and oxidative addition on a Pd center [8–10], olefin insertion into M–H bonds [11], and catalytic oxidation–reduction hydration of olefins via Co(diketonato)$_2$ [12]. It has been demonstrated also that the enantioselectivity (*ee*) of catalytic hydrogenation, cyclopropanation, and epoxidation may depend significantly on the electronic nature of the substituent on chiral auxiliary ligands [13–17]. Significant tuning of the metal–ligand charge transfer excited states in the Pt/Ru complexes of 2,2′-bipyridine has also been achieved [18–20]. Substituent-regulated ground-state electron transfer can also be advantageous in probing fast electron transfer on the time-scale of infrared spectroscopy [21]. For mononuclear coordination compounds, variation of substituents away from the first coordination sphere has become a versatile tool in optimizing molecular properties; in conjunction with the linear free energy relationships (LFER) therein, precise control is achievable.

In contrast to the above-mentioned progress in the understanding of substituent effects of mononuclear compounds, little is known about such effects in metal–metal bonded dinuclear compounds [22]. In fact, there were only a handful of examples prior to our recent studies, and the linear free energy relationships therein were sometimes inexplicit [23–28]. With the ever-expanding scope of the applications of dinuclear compounds and their supra-molecular assemblies [29], a systematic elucidation of the substituent effect and LFER becomes necessary. A potentially important application of such a relationship is to carbene-transfer reactions catalyzed by dirhodium tetracarboxylates and their analogs [30–32], where it has been recognized recently that the electrophilicity of the metallo-carbenoid intermediate, and hence the chemo- and regio-selectivities, may be regulated via the electronic effects of the bridging ligands [28,33,34].

Our recent work has been focused on the fine-tuning of molecular properties of dinuclear compounds through substituents and the resultant LFER. Diarylformamidine (Scheme 1) was chosen as the bridging ligand due to (i) the documented capacity of the ligand to support dinuclear paddlewheel compounds with a variety of metal centers [22,35,36] and (ii) the facile synthesis of derivatives with a broad range of electron-releasing and -withdrawing substituents [37,38].

2. Synthesis and molecular structures

2.1. Synthesis

Preparation of tetrakis(μ-diarylformamidinato)dimetals ($M_2(\text{form})_4(L_{ax})_m$, where form is the generic diarylformamidinate, and L_{ax} is the axial ligand, and $m = 0-2$) is generally straightforward, and the synthetic route utilized depends on the starting materials available for individual metal centers. Crystalline $Mo_2(\text{form})_4$ with ligands **L1–L11** can be obtained in high yield either by refluxing $Mo(CO)_6$ with excess formamidine in *o*-dichlorobenzene, or by stoichiometric ligand metathesis between $Mo_2(O_2CCH_3)_4$ and the lithiated formamidine [39–41]. The reaction between molten formamidine and $M_2(OAc)_4(L_{ax})_m$ is a facile and high-yield route to $Ru_2(\text{form})_4Cl$ with **L1–L10** [42–44], $Re_2(\text{form})_4Cl_2$ with **L1–L7, L10** [45,46], and $Rh_2(\text{form})_4$ (**L1–L10**) [47,48]. Alternatively, stoichiometric ligand metathesis can be

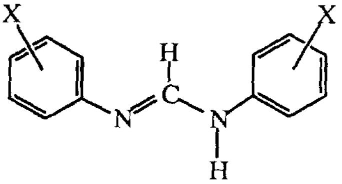

X (σ)

L1: *p*-OMe (-0.27)
L2: *p*-Me (-0.17)
L3: H (0)
L4: *m*-OMe (0.12)
L5: *p*-Cl (0.23)
L6: *m*-Cl (0.37)
L7: *m*-CF_3 (0.43)
L8: *p*-CF_3 (0.54)
L9: 3,4-Cl_2 (0.60)
L10: 3,5-Cl_2 (0.74)
L11: *p*-COMe (0.50)

Scheme 1. Substituted diphenylformamidine, and the nature, position, and Hammett constant of the phenyl substituent.

accomplished by reacting the tetraacetate species with formamidine in the presence of Et_3N, as in the case of $Ru_2(form)_4Cl$ [44]. Refluxing the formamidine with $RhCl_3$ in the presence of either Et_3N or NaOMe led to the formation of $Rh_2(form)_4$ [48], but side reactions yielded also diarylazo compounds (ArNNAr) via cleavage of formamidine. $Rh_2(form)_4$ can be prepared also by treating $Rh_2(form)_2(O_2CCF_3)_2$ with the lithiated formamidine [49]. $Ni_2(form)_4$ (**L1**–**L10**) is synthetically accessible either via the reaction between anhydrous NiX_2 ($X = Cl$, Br) and the lithiated formamidine in low yield [50,51], or by treating *cis*-$Ni(\eta^1\text{-Hform})_2Cl_2$ with Li–*n*-Bu in an unspecified yield [52]. The optimal route appears to be the pyrolysis of *trans*-$Ni(\eta^2\text{-form})_2(py)_2$ [51]. $W_2(form)_4$ can be obtained by the low temperature reaction between the lithiated formamidine and $[W_2Cl_8]^{4-}$, which was generated by the reduction of WCl_4 with either Na/Hg or $Na[HBEt_3]$ [35,53]. The monocarbonyl adducts of $Rh_2(form)_4$ were formed in situ by bubbling CO gas through a solution of $Rh_2(form)_4$, and could be isolated as crystalline solids in most cases [48,49]. The mono- and bis-phenylacetylide adducts of $[Ru_2(form)_4]^{1+/2+}$ core (mono-adduct with **L3**, **L5**–**L10**; bis-adduct with **L1**, **L3**, **L5**-**L10**) were generated by controlled post-synthesis treatment of $[Ru_2(form)_4(C{\equiv}CPh)_2]^-$ intermediate [43,54,55], which was formed by treating $Ru_2(form)_4Cl$ with a large excess (= 50 fold) of $LiC{\equiv}CPh$. In general, neither the yield nor the purification for all the dinuclear species discussed here appears dependent on the electronic nature of the phenyl substituent. A brief summary of dinuclear compounds supported by formamidinate, including some metal centers not mentioned above, can also be found in a recent publication [36].

2.2. Structures

Similar to the dinuclear compounds supported by ligands iso-electronic to formamidinate, such as carboxylate, carboxamidate, and triazenate [22], all the aforementioned dinuclear compounds adopt the paddlewheel motif (Scheme 2). To explore substituent perturbation of the molecular structure, and especially the coordination geometry around the dinuclear core, single crystal X-ray diffraction studies were carried out for a few compounds from each series, typically those with substituents of drastically different electronic effects. In the case of $Mo_2(form)_4$, structural study of the compounds with ligands **L1**–**L3**, **L6**, and **L10** [39,41] reveals that both the Mo–Mo and Mo–N bond lengths are within narrow ranges of 2.085–2.097 Å and 2.155–2.171 Å, respectively. For the dinickel analogs, the Ni–Ni and Ni–N distances for the compounds with ligands **L2**, **L3**, and **L10** are 2.462–2.490 Å and 1.904–1.917 Å, respectively [50–52]. Comparison of the structural data for dirhodium compounds of ligands **L2**-**L4** and **L10** [47–49] also reveals only minute deviations for both the Rh–Rh (2.415–2.458 Å) and Rh–N (2.041–2.055 Å) bond lengths. Similar trends have also been confirmed for the diruthenium series of general formulas $Ru_2(form)_4Cl$, $Ru_2(form)_4(C{\equiv}CPh)$, and $Ru_2(form)_4(C{\equiv}CPh)_2$ [42–44,54,55]. Table 1 summarizes the key structural parame-

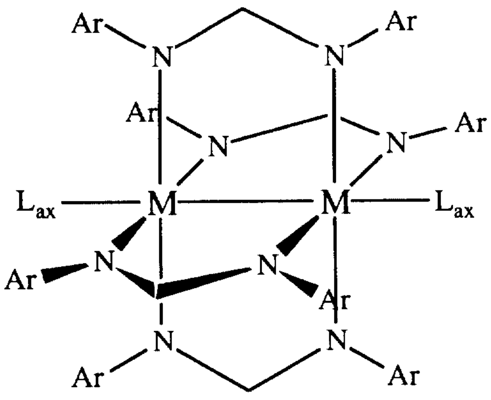

Scheme 2. Paddlewheel motif for $M_2(form)_4(L_{ax})_2$.

ters determined for $M_2(form)_4(L_{ax})_m$ series with more than three known structures. The minimal changes at the first coordination sphere of the M_2 core clearly indicate that variation in the electronic nature of phenyl substituents does not alter the nature of either M–M or M–N bonding to any significant degree.

3. Electrochemical characterizations

3.1. LFER derived from electrochemical studies

Substituent effects in organic chemistry are quantified as a linear free energy relationship, via the Hammett equation:

$$\Delta(\Delta G) = RT\,\Delta(\log \kappa) = RT \log \frac{\kappa}{\kappa^{\circ}} = \rho\sigma \qquad (1)$$

where ΔG is Gibbs energy, κ is either the rate (k) or the equilibrium constant (K), $^{\circ}$ denotes the unsubstituted species, and ρ and σ are, respectively, the reaction and substituent (Hammett) constants [1–4]. Less often is the analogous equation expressed in terms of electrode potentials (E° or $E_{1/2}$) [56]. For coordination and organometallic compounds, however, Hammett relationships based on redox potentials appear more common than those based on either kinetic or non-redox thermodynamic parameters. This is clearly attributed to the flexibility in oxidation states common to all the transition metal ions, which renders reversible redox couples accessible over a broad potential window.

The aforementioned dinuclear compounds supported by formamidinate ligands are no exception: all of them undergo at least one of the four one-electron redox steps outlined below.

$$M_2(I,\ II) \underset{\substack{-e^-\\ A}}{\overset{-e^-}{\rightleftharpoons}} M_2(II,\ II) \underset{\substack{-e^-\\ B}}{\overset{-e^-}{\rightleftharpoons}} M_2(II,\ III) \underset{\substack{-e^-\\ C}}{\overset{-e^-}{\rightleftharpoons}} M_2(III,\ III) \underset{\substack{-e^-\\ D}}{\overset{-e^-}{\rightleftharpoons}} M_2(III,\ IV)$$

The rich redox chemistry thus enables the establishment of an LFER between the measured half-wave potential ($E_{1/2}$)[1] and σ through a modified Hammett equation [56]:

Table 1
Key bond lengths observed around the dinuclear core for $M_2(\mathrm{form})_4(L_{ax})_m$

Mo_2(form)$_4$				
X	Mo–Mo (Å)	Mo–N (Å)		
p-OMe[a]	2.0964	2.158		
p-Me[b]	2.085	2.171		
H[a]	2.0944	2.155		
m-Cl[a]	2.0958	2.161		
3,5-Cl_2 [a]	2.0965	2.166		
Rh_2(form)$_4$				
X	Rh–Rh (Å)	Rh–N (Å)		
p-Me[c]	2.434	2.050		
H[d]	2.457	2.048		
m-MeO[e]	2.4518	2.048		
3,5-Cl_2 [e]	2.4581	2.053		
Ni_2(form)$_4$				
X(σ)	Ni–Ni (Å)	Ni–N (Å)		
p-Me[f]	2.485	1.904		
H[g]	2.490	1.913		
3,5-Cl_2 [h]	2.462	1.917		
Ru_2(form)$_4$Cl				
X	Ru–Ru (Å)	Ru^{3+}–Cl (Å)	Ru^{3+}–N (Å)	Ru^{2+}–N (Å)
p-OMe[i]	2.390	2.433	2.080	2.059
m-Me[j]	2.370	2.412	2.092	2.030
H[k]	2.339	2.414	2.090	2.044
m-MeO[i]	2.386	2.432	2.077	2.030
3,5-Cl_2 [i]	2.369	2.395	2.089	2.054
Ru_2(form)$_4$(C≡CPh)				
X	Ru–Ru (Å)	Ru^{3+}–C (Å)	Ru^{3+}–N (Å)	Ru^{2+}–N (Å)
H[k]	2.369	2.037	2.114	2.048
m-Cl[l]	2.387	2.057	2.113	2.052
3,5-Cl_2 [l]	2.369	2.036	2.082	2.034

[a] Structural data were taken from Refs. [41];
[b] [39]; [c] [49]; [d] [47]; [e] [48]; [f] [50]; [g] [52]; [h] [51]; [i] [59]; [j] [42]; [k] [43]; [l] [55].

---

[1] It is well known that the measured electrode potentials can be significantly influenced by the solvents, supporting electrolytes, concentration, and the temperature. All the measurements of the cited electrode potentials were conducted in CH_2Cl_2 with $(n\text{-}Bu)_4NBF_4$ as the supporting electrolyte, Pt working and auxiliary electrodes, Ag | AgCl reference electrode, scan rate 100 mV s^{-1}, and temperature range of 23–25°C; Under these conditions, the $E_{1/2}(Fc^+/Fc)$ was consistently measured at + 625 mV. Typical $[M_2]$ is about 1 mM.

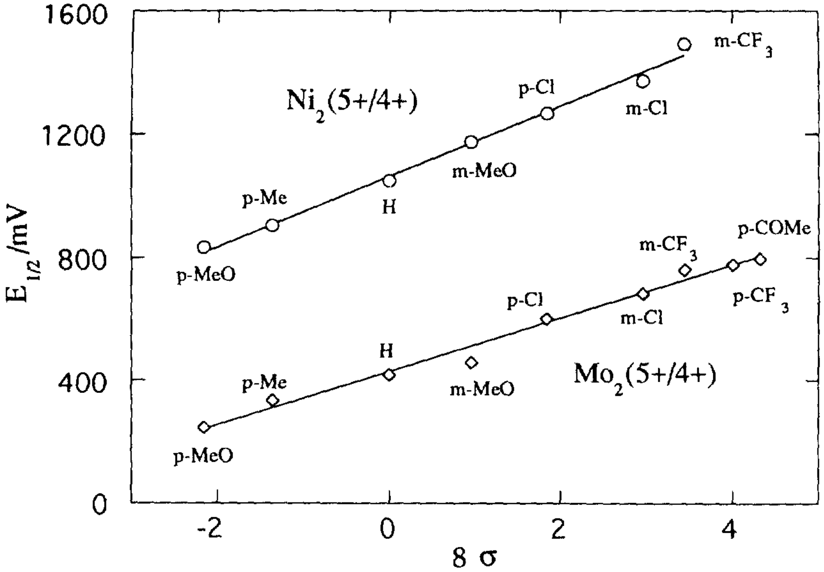

Fig. 1. Hammett plot of $E_{1/2}(5+/4+)$ versus 8σ for both the $Mo_2(form)_4$ and $Ni_2(form)_4$ series.

$$\Delta E_{1/2} = E_{1/2}(X) - E_{1/2}(H) = \rho(8\sigma) \tag{2}$$

where $E_{1/2}(H)$ and $E_{1/2}(X)$ are the half-wave potentials for the dinuclear species supported by unsubstituted and substituted formamidinates, respectively, and the numeric coefficient 8 is the number of substituted phenyl rings per dinuclear compound.

For both the dimolybdenum(II,II) (Mo–Mo quadruply bonded) and dinickel(II,II) (no Ni–Ni bond) series, the one-electron oxidation (step B) is the only redox couple observed and is (quasi)reversible for most compounds [41,51]. Linear least-squares fittings according to Eq. (2) yield $\rho(Mo_2)$ of 85 mV and $\rho(Ni_2)$ of 114 mV, and the linear plots are shown in Fig. 1. In contrast, the isostructural dirhodium(II,II) (Rh–Rh single bond) series displays three consecutive one electron processes: one reduction (step A) and two oxidations (steps B and C) [48]. All the redox couples for dirhodium species are reversible, and the linear fit of $E_{1/2}$ versus 8σ according to Eq. (2) resulted in the reaction constants ρ as 97 mV for $Rh_2(4+/3+)$ (A), 98 mV for $Rh_2(5+/4+)$ (B), and 96 mV for $Rh_2(6+/5+)$ (C), which are identical within experimental errors. Singly-bonded $Ru_2(form)_4(C{\equiv}CPh)_2$ organometallic species also undergo three one-electron processes, i.e. steps B–D [54]; the respective reaction constants are 81, 92, and 72 mV, and the corresponding $E_{1/2}$ versus 8σ linear plots are shown in Fig. 2. Since the accuracy of $E_{1/2}$ values is generally assured by the (quasi)reversibility of the redox couples observed for the above-mentioned series, the correlation coefficient is always greater than 98%, indicating excellent correlation between $E_{1/2}$ and σ[2].

---

[2] Generally, linear correlation is considered excellent when $R \geq 0.99$, satisfactory when $0.98 \geq R \geq 0.95$, and fair when $0.95 > R \geq 0.90$. See p. 105 of Ref. [2] for more detailed discussion.

The coupling between the electrode reaction and subsequent chemical reactions results in somewhat complicated behavior for the $Ru_2(form)_4X$ series, where X is either Cl^- or $PhC{\equiv}C^-$. For the $Ru_2(form)_4Cl$ series (Ru–Ru bond order 2.5), steps B and C are observed. While C is quasireversible, only the cathodic wave of B is observed for all the compounds [44]. The reaction constants (correlation coefficients) determined from fittings of $E_{pc}(B)$ and $E_{1/2}(C)$ versus σ are 69.9 (0.98) and 90.4 (0.99) mV, respectively. In the $Ru_2(form)_4(C{\equiv}CPh)$ series (bond order 2.5), the one-electron reduction (step B) appears reversible for all the compounds, and the corresponding reaction constant is 82 mV [55]. The oxidation couple (C) has been observed for several compounds from the series, while the disappearance of C in other compounds is currently being investigated.

3.2. Choice of Hammett constants

For all the series investigated so far, satisfactory fittings according to Eq. (2) were achieved with the Hammett σ-constants (σ_m and σ_p) based on the ionization of benzoic acid [1]. To examine if significant conjugation between the phenyl-substituent and the dinuclear core exists [2], fittings with both σ^- and σ^+ constants were also attempted. The correlation coefficients were no better than 0.97 [41], which clearly indicates the absence of dominant resonance contribution from the substituent in our systems. This result is not very surprising, since the phenyl group has rotational freedom in respect to the first coordination sphere of the dinuclear core, which eliminates any significant contribution through conjugation. MO studies of both dimolybdenum and dinickel systems have confirmed the absence of direct orbital contributions to either the HOMO or the LUMO from the substituent groups [41,57].

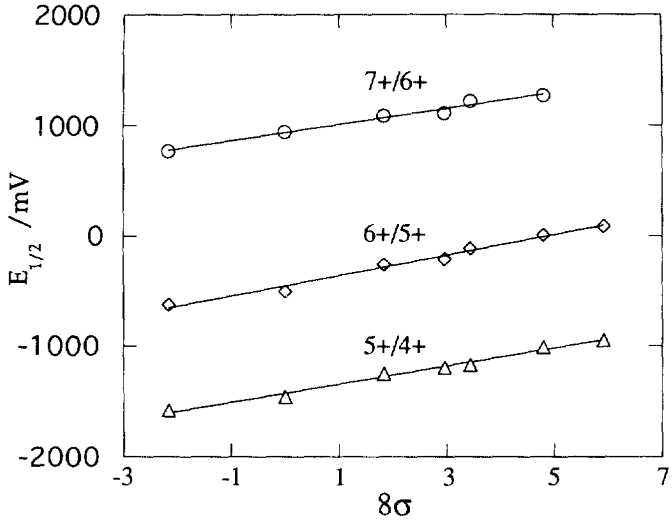

Fig. 2. Hammett plots of $E_{1/2}$ versus 8σ for (7+/6+), (6+/5+), and (5+/4+) couples of the $Ru_2(form)_4(C{\equiv}CPh)_2$ series.

3.3. Discussion

Several trends that have emerged from the linear correlation between $E_{1/2}$ and σ are worthy of elaboration. Since the oxidation and reduction processes correspond respectively to the removal of an electron from the HOMO and the addition of an electron to the LUMO, the satisfactory correlation between the corresponding electrode potentials and Hammett constants clearly indicates that the energies of frontier orbitals of dinuclear species can be tuned precisely through phenyl substitution. The range of tuning can be significant, as shown in Table 2. In fact, the potential range of 900 mV for the dinickel series [51] is among the largest known for a homologous series of metal complexes. Furthermore, when the one-electron oxidation and reduction couples are both observed for a neutral molecule, the following approximate relationship exists:

$$E_{1/2}(\text{oxidation}) - E_{1/2}(\text{reduction}) = \text{E(LUMO)} - \text{E(HOMO)} \qquad (3)$$

where both the E(LUMO) and E(HOMO) refer to the solvated molecule, and the error that results from neglecting the difference in both diffusion and activity coefficients among neutral, reduced, and oxidized species is small (generally less than 10 mV) [58]. The electrochemical HOMO–LUMO gap has been calculated for several series investigated, and the mean value within each series is listed in Table 2. As noted in Table 2, the estimated standard deviation (estimate S.D.) for a HOMO–LUMO gap is generally less than 5% of the gap itself, which clearly indicates that the HOMO–LUMO gap is relatively invariant within each series.

Also of interest is the comparison of the $\rho(M_2(5+/4+))$ values obtained for the isostructural dimolybdenum, dirhodium, and dinickel series: a gradual increase is observed as one moves across the periodic table from left to right. This is opposite to the trend observed for metal-based redox couples in metallotetraphenylprophyrins [5], and the contrast may be attributed to the difference in the metal-based orbitals involved.

4. Spectroscopy

4.1. UV–vis absorption spectra

While the absolute energies of the HOMO and sometimes that of the LUMO can be inferred from electrode potentials, energy information of other valence orbitals cannot be similarly assessed. Nevertheless, the dinuclear compounds discussed generally display multiple absorptions in both the UV and visible regions, and the HOMO is always involved in at least one of the observed transitions. Therefore, the substituent-dependence of other valence orbitals may be inferred through the comparison of the peak positions across a homologous series.

For the dimolybdenum(II,II) compounds [41], almost identical δ–δ^* transition energies (ranging from 2.78–2.88 eV) were observed across the series, suggesting an identical HOMO–LUMO gap for all of the compounds. Therefore, the substituent

Table 2
Electrochemical and spectroscopic parameters for $M_2(form)_4(L_{ax})_m$

Entry	ρ(step A), ΔE [a] (mV)	ρ(step B), ΔE (mV)	ρ(step C), ΔE (mV)	ρ(step D), ΔE (mV)	$[E(ox)-E(red)]/V$ [b] (estimated S.D.)
$Mo_2(form)_4$	–	87, 780	–	–	–
$Ru_2(form)_4Cl$	–	70, 520	90, 690	–	1.33(7)
$Ru_2(form)_4(C{\equiv}CPh)$	–	82, 660	–	–	1.22(2)
$Ru_2(form)_4(C{\equiv}CPh)_2$	–	72, 630	92, 710	81, 640	1.35(6)
$Rh_2(form)_4$	97, 710	98, 760	96, 720		1.57(4)
$Ni_2(form)_4$	–	114, 900	–	–	–

[a] ρ, the reaction constant defined in Eq. (2); ΔE, the potential tuning range, which is the difference between the most and the least positive electrode potentials for the same redox couple.

[b] Electrochemical HOMO–LUMO gap as defined by Eq. (3)

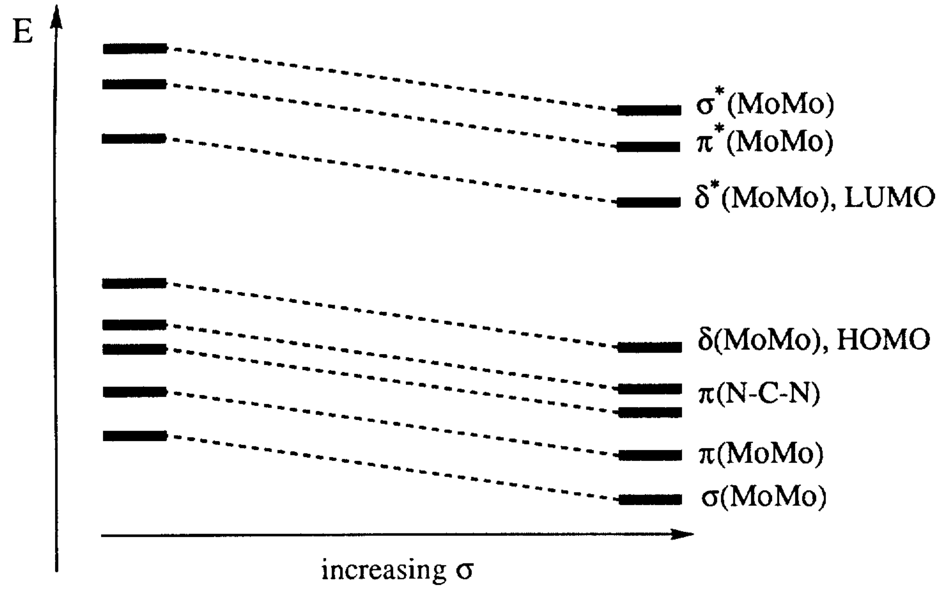

Scheme 3. Substituent dependence of energies of upper valence orbitals in $Mo_2(form)_4$.

dependence of the E(LUMO), should be the same as that of the E(HOMO), resulting in a parallel shift of frontier orbitals. Similarly, the λ_{max} of the ligand-to-metal charge transfer (LMCT) transitions were also found to be substituent-independent, extending the parallel shift to other high energy occupied valence orbitals. These observations of substituent perturbation are summarized by a qualitative MO scheme (Scheme 3). With the same trend observed for the series of $Ni_2(form)_4$ [51], $Rh_2(form)_4$ [48], $Ru_2(form)_4(C{\equiv}CPh)$ [55], and $Ru_2(form)_4(C{\equiv}CPh)_2$ compounds [54], one can conclude that for most $M_2(form)_4(L)_m$ species studied to date, the electron withdrawal/donation by the phenyl substituent induces a uniform stabilization/destabilization on all the upper valence orbitals, while the relative distribution of these orbitals is unchanged.

The only exception to the parallel shift of frontier orbitals occurs in the $Ru_2(form)_4Cl$ series [44], where the absorption band of the lowest transition energy blue-shifts as the σ increases, and fitting of the transition energy according to $\Delta E(\text{transition}) = \rho(8\sigma)$ yielded a ρ value of 260 cm^{-1}. The origin of this linear dependence is currently under investigation.

4.2. IR spectra

Orbital interaction between the dinuclear center and axially-bonded unsaturated organic functional groups is of great interest, since such an interaction is key to the electrophilicity of an axially-bonded carbene in carbene-transfer reactions promoted by dirhodium and diruthenium paddlewheel compounds [30–32,59]. The possible

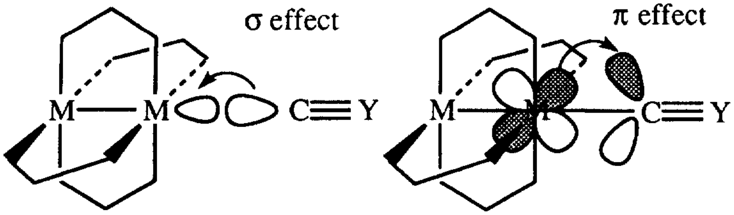

Scheme 4. Activation of axial substrate.

control of this interaction by the substituents has been examined via analysis of IR spectroscopic data for several series. Activation of an axial substrate by a dinuclear center may involve two mechanisms: (i) weakening of the C–Y σ-bond through the formation of a strong M–C σ bond (σ-effect, also known as *trans*-influence) and (ii) weakening of the C–Y π-bond through d_π–π^* back-donation (Y is the atomic center trans to M), as shown in Scheme 4. When the first mechanism is operative, the stretching frequency ν(C–Y) should decrease with increasing σ since the dinuclear center becomes more electron deficient and a stronger σ(M–C) bond results. Alternatively, ν(C–Y) should increase with increasing σ for the second mechanism since there is less electron density donated from the dinuclear core.

For the series of $Ru_2(form)_4(C{\equiv}CPh)$, the $\nu(C{\equiv}C)$ decreases with increasing σ, and fitting according to $\Delta\nu = \rho(8\sigma)$ results in a ρ value of $-3.7\ cm^{-1}$ [55]. The negative ρ value clearly indicates that the σ-effect is dominant. On the other hand, the ν(CO) for the CO adduct of $Rh_2(form)_4$ increases with the increasing σ, and the fitting yields a ρ value of $+3.2\ cm^{-1}$ [48], which unambiguously points to a strong π-back-donating effect by a dirhodium(II,II) core. Interestingly, a nearly identical $\nu(C{\equiv}C)$ was observed for all the $Ru_2(form)_4(C{\equiv}CPh)_2$ compounds, indicating the equal contribution of both σ- and π-effects [54].

5. Other related studies

The earliest attempt in elucidating the LFER of dinuclear paddlewheel species was carried out by Bear and Kadish [26], who explored the dependence of $E_{1/2}((Rh_2(O_2CR)_4)^{+/0})$ (recorded in DMF with a SCE reference electrode) on the nature of the alkyl group (R). Fitting of $E_{1/2}$ according to the Hammett equation $\Delta E_{1/2} = 4\sigma\rho$ results in a reaction constant of 67 mV. Subsequently, a similar relationship was confirmed by variation of the substituents on pyridine axially bonded to the dirhodium core [27]. More recently, Pirrung probed the substituent effect in $Rh_2(O_2CR)_4$ promoted intramolecular carbene insertion of methyl 2-diazo-3-oxo-6-(2-propenyloxy)hexanoate [28]. The linear free energy relationships describing both regio- and chemo-selectivities are of the general form $\Delta(\Delta G^{\neq}) = \text{constant} + \rho\sigma^{\dagger}$, where σ^{+} is a combination of polarizability (σ_I) and field (σ_F) effects for R as alkyl, and a combination of σ_I, σ_F, and resonance (σ_R) effects for R as aryl. Interestingly, the resonance contribution is the most dominant in the

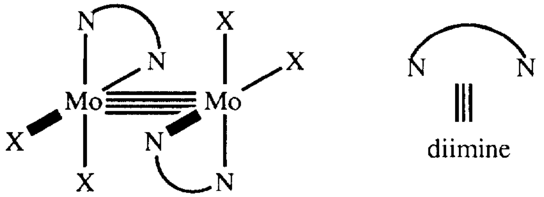

Scheme 5. Porposed structure for α-$Mo_2X_4(diimine)_2$.

latter case (benzoates as the bridging ligands), although the orbital origin is uncertain[3].

Although no explicit LFER was revealed for dinuclear species containing M–M multiple bonds prior to our work, the stereo-electronic effect of substituents was demonstrated by Cotton et al. [24,25]. Through a variation of the R group of PR_3, a linear correlation between the $E_{1/2}(Mo_2^{5+/4+})$ for $Mo_2X_4(PR_3)_4$ and the π-acidity of PR_3 (measured by both the $\nu(CO)$ and $\delta(^{13}CO)$ of $Ni(CO)_3(PR_3)$) was established. Substituent effects in the complexes of the general formula $Cr_2(O_2CR)_4(4\text{-}Xpy)_2$ (R = $C(CH_3)_3$, CH_3, H, $CClH_2$, or CHF_2; X = NH_2, $N(CH_3)_2$, $C(CH_3)_3$ and CN) were probed by Cotton and Wang, where, among other interesting findings, Cr–Cr distance was found to be linearly dependent on both the pK_a of the pyridine (positive slope) and the pK_a of carboxylic acid (negative slope) [23]. Contemporary to our work, Chisholm et al. noted that the absorption maximum of the $\delta \rightarrow \delta^*$ transition for $Mo_2(O_2CAr)_4$ with Ar as nitro-substituted phenyls can be significantly red-shifted from that of $Mo_2(O_2CPh)_4$, although no quantitative correlation between $E(\delta \rightarrow \delta^*)$ and the electronic nature of bridging ligands was revealed [60].

An interesting series of the general formula α-$Mo_2X_4(\eta^2\text{-diimine})_2$ (Scheme 5) was investigated by Baird and Dunbar [61], where both the energy and intensity of the $\delta - \delta^*$ transition were found to correlate with the $E_{1/2}$ of the one electron reduction couple of the free diimine. This is in stark contrast with our result for $Mo_2(form)_4$, where almost identical UV–vis spectra were observed across the series. The discrepancy may be attributed to (i) coupling between π(Mo–Mo) and π(imine) orbitals enabled by the chelating geometry of the imine or (ii) direct coordination of the hetero-cycle to the Mo center, and may be resolved when the X-ray structure of α-$Mo_2X_4(\eta^2\text{-diimine})_2$ becomes available. This series of compounds may also become the key link in the interpretation of the electrochemical and spectroscopic data for dinuclear species with Lever's parameter $E_L(L)$, which is largely based on the linear regression of electrochemical and spectroscopic data for $M(diimine)(L')_2$ complexes [62,63]. To date, lack of a sufficient number of dinuclear species containing diimine ligands prohibits a meaningful application of Lever's parameter.

---

[3] It was suggested by Pirrung that the pronounced resonance effect is the result of the direct coupling between the π-donor orbitals delocalized within the benzoate group and the π* of dirhodium core. However, such an orbital mixing is symmetry-forbidden. The metal-centered orbital shown in Figure 20 of Ref. [18] is in-fact the δ-type orbital of Rh_2, instead of the π* orbital Pirrung had assumed.

The intricacy of M_2-core-substrate interactions has been demonstrated by Chisholm recently, where a U-type Hammett plot ($\log(k/k_H)$ vs. σ) was obtained for the rate (k) of reductive cleavage of thiobenzophenone ($Ar_2C{=}S$) by $Mo_2(OCH_2t\text{-}Bu)_6$ [64]. This behavior was interpreted as the lack of charge build-up in the transition state, although the possibility of competing mechanisms, a common rationale for concave Hammett plots [2], cannot be excluded.

6. Conclusion

It has been demonstrated through electrochemical studies that the energy levels of the frontier orbitals for the dinuclear species can be precisely tuned by varying the electronic nature of the substituent at the ligand periphery. Meanwhile, a minimal substituent-dependence for the valence structure of the dinuclear core is implied by a constant electronic absorption spectrum within a homologous series. Moreover, the tunings of orbital energies are significant: 600–900 mV in electrode potential and ca. 60–90 kJ mol^{-1} in $\Delta(\Delta G°)$ (cf. Nernst equation). What remains to be investigated is how much the tuning in the ground state ($\Delta(\Delta G°)$) will be imparted into the tuning in the transition state ($\Delta(\Delta G^{\neq})$). Namely, what exactly is the value of m in the general linear free energy relationship (Eq. (4)) for dinuclear species?

$$\log\left(\frac{K}{K°}\right) = m \log\left(\frac{k}{k°}\right) \tag{4}$$

We are currently exploring the implications of the LFER in the general reactivity of paddlewheel species, and in their catalytic applications in carbene, nitrene, and oxo-transfer reactions.

Acknowledgements

Financial support is provided by the Petroleum Research Fund/ACS, Florida Solar Energy Center, and the Department of Chemistry, Florida Institute of Technology. I owe a great debt to my collaborators, and especially to Dr Chun Lin, who was instrumental in carrying out the majority of experimental work described here. Insightful discussion with Professors Alan B. Brown and Judith L. Eglin are also appreciated deeply.

References

[1] L.P. Hammett, Physical Organic Chemistry, McGraw-Hill, New York, 1970.
[2] J. Shorter, Correlation Analysis in Organic Chemistry, Clarendon Press, Oxford, 1973.
[3] R.W. Taft (Ed.), Progress in Physical Organic Chemistry, vol. 16, Wiley, New York, 1987.
[4] C. Hansch, A. Leo, R.W. Taft, Chem. Rev. 91 (1991) 165.

[5] K.M. Kadish, Prog. Inorg. Chem. 34 (1986) 435.
[6] D. Dolphin, T.G. Traylor, L.Y. Xie, Acc. Chem. Res. 30 (1997) 251.
[7] D. Ostovic, T.C. Bruice, Acc. Chem. Res. 25 (1992) 314.
[8] D. Baranano, J.F. Hartwig, J. Am. Chem. Soc. 117 (1995) 2937.
[9] M.S. Driver, J.F. Hartwig, J. Am. Chem. Soc. 119 (1997) 8232.
[10] A. Jutand, A. Mosleh, Organometallics 14 (1995) 1810.
[11] B.J. Burger, B.D. Santarsiero, M.S. Trimmer, J.E. Bercaw, J. Am. Chem. Soc. 110 (1988) 3134.
[12] K. Kato, T. Yamada, T. Takai, S. Inoki, S. Isayama, Bull. Chem. Soc. Jpn. 63 (1990) 179.
[13] T.V. RajanBabu, T.A. Ayers, G.A. Halliday, K.K. You, J.C. Calabrese, J. Org. Chem. 62 (1997) 6012.
[14] S.-B. Park, K. Murata, H. Matsumoto, H. Nishiyama, Tetrahedron: Asymmetry 6 (1995) 2487.
[15] T.V. Rajanbabu, T.A. Ayers, A.L. Casalnuovo, J. Am. Chem. Soc. 116 (1994) 4101.
[16] A.L. Casalnuovo, T.V. Rajanbabu, T.A. Ayers, T.H. Warren, J. Am. Chem. Soc. 116 (1994) 9869.
[17] E.N. Jacobsen, W. Zhang, M.L. Guler, J. Am. Chem. Soc. 113 (1991) 6703.
[18] K. Kalyanasundaram, S.M. Zakeeruddin, M.K. Nazeeruddin, Coord. Chem. Rev. 132 (1994) 259.
[19] K. Kalyanasundaram, Photochemistry of Polypyridine and Porphyrin Complexes, Academic Press, London, 1992.
[20] S.D. Cummings, R. Eisenberg, J. Am. Chem. Soc. 118 (1996) 1949.
[21] T. Ito, T. Hamaguchi, H. Nagino, T. Yamguchi, J. Washington, C.P. Kubiak, Science 277 (1997) 660.
[22] F.A. Cotton, R.A. Walton, Multiple Bonds between Metal Atoms, Oxford University Press, Oxford, 1993.
[23] F.A. Cotton, W. Wang, Nouv. J. Chim. 8 (1984) 331.
[24] F.A. Cotton, L.M. Daniels, G.L. Powell, A.J. Kahaian, T.J. Smith, E.F. Vogel, Inorg. Chim. Acta 144 (1988) 109.
[25] D.S. Hanselman, T.J. Smith, Polyhedron 7 (1988) 2679.
[26] K. Das, K.M. Kadish, J.L. Bear, Inorg. Chem. 17 (1978) 930.
[27] L.A. Bottomley, T.A. Hallberg, Inorg. Chem. 23 (1984) 1584.
[28] M.C. Pirrung, A.T. Morehead, J. Am. Chem. Soc. 116 (1994) 8991.
[29] Recent interesting applications include, (a) Nonlinear optical effect: K. Mashima, M. Tanaka, Y. Kaneda, A. Fukumoto, H. Mizomoto, K. Tani, H. Nakano, Chem. Lett. (1997) 411. (b) Inorganic liquid crystals: D.V. Baxter, R.H. Cayton, M.H. Chisholm, J.C. Huffman, E.F. Putilina, S.L. Tagg, J.L. Wesemann, J.W. Zwanziger, F.D. Darrington, J. Am. Chem. Soc. 116 (1994) 4551. (c) One dimensional polymers: G.M. Finniss, E. Canadell, C. Campana, K.R. Dunbar, Angew. Chem. Int. Ed. Engl. 35 (1996) 2772. (d) Antitumor agents: K.V. Catalan, D.J. Mindiola, D.L. Ward, K.R. Dunbar, Inorg. Chem. 36 (1997) 2458.
[30] M.P. Doyle, M.A. McKervey, Chem. Comm. (1997) 983
[31] M.P. Doyle, Aldrichim. Acta 29 (1996) 3.
[32] A. Padwa, D.J. Austin, Angew. Chem. Int. Ed. Engl. 33 (1994) 1797.
[33] M.P. Doyle, L.J. Westrum, W.N.E. Wolthuis, M.M. See, W.P. Boone, V. Bagheri, M.M. Pearson, J. Am. Chem. Soc. 115 (1993) 958.
[34] A. Padwa, D.J. Austin, A.T. Price, M.A. Semones, M.P. Doyle, M.N. Protopopova, W.R. Winchester, A. Tran, J. Am. Chem. Soc. 115 (1993) 8669.
[35] F.A. Cotton, T. Ren, J. Am. Chem. Soc. 114 (1992) 2237.
[36] F.A. Cotton, S.C. Haefner, A.P. Sattelberger, Inorg. Chem. 35 (1996) 7350.
[37] J. Barker, M. Kilner, Coord. Chem. Rev. 133 (1994) 219.
[38] W. Bradley, I. Wright, J. Chem. Soc. (1956) 640.
[39] F.A. Cotton, X. Feng, M. Matusz, Inorg. Chem. 28 (1989) 594.
[40] C. Lin, J.D. Protasiewicz, E.T. Smith, T. Ren, J. Chem. Soc., Chem. Commun. (1995) 2257.
[41] C. Lin, J.D. Protasiewicz, E.T. Smith, T. Ren, Inorg. Chem. 35 (1996) 6422.
[42] F.A. Cotton, T. Ren, Inorg. Chem. 34 (1995) 3190.
[43] J.L. Bear, B. Han, S. Huang, K.M. Kadish, Inorg. Chem. 35 (1996) 3012.
[44] C. Lin, T. Ren, E.J. Valente, J.D. Zubkowski, E.T. Smith, Chem. Lett. (1997) 753.
[45] F.A. Cotton, T. Ren, J. Am. Chem. Soc. 114 (1992) 2495.

[46] J.L. Eglin, T. Ren, in preparation.
[47] J.L. Bear, C.-L. Yao, R.S. Lifsey, J.D. Korp, K.M. Kadish, Inorg. Chem. 30 (1991) 336.
[48] T. Ren, C. Lin, E.J. Valente, J.D. Zubkowskic, in preparation.
[49] P. Piraino, G. Bruno, S.L. Schiavo, F. Laschi, P. Zanello, Inorg. Chem. 26 (1987) 2205.
[50] F.A. Cotton, M. Matusz, R. Poli, X. Feng, J. Am. Chem. Soc. 110 (1988) 1144.
[51] C. Lin, J.D. Protasiewicz, T. Ren, Inorg. Chem. 35 (1996) 7455.
[52] D.I. Arnold, F.A. Cotton, D.J. Maloney, J.H. Matonic, C.A. Murillo, Polyhedron 16 (1997) 133.
[53] J.L. Eglin, Personal communication.
[54] C. Lin, T. Ren, E.J. Valente, J.D. Zubkowskic, J. Chem. Soc. Dalton Trans. (1998) 571.
[55] C. Lin, T. Ren, E.J. Valente, J.D. Zubkowskic, J. Organomet. Chem., submitted for publication.
[56] P. Zuman, The Elucidation of Organic Electrode Processes, Academic Press, New York, 1969.
[57] C. Lin, PhD dissertation, Florida Institute of Technology, 1997.
[58] R.O. Loutfy, R.O. Loutfy, Can. J. Chem. 54 (1976) 1454.
[59] A.F. Noels, A. Demonceau, E. Carlier, A.J. Hubert, R.-L. Marquez-Silva, R.A. Sanchez-Delgado, J. Chem. Soc. Chem. Commun. (1988) 783.
[60] M.H. Chisholm, J.C. Huffman, S.S. Iyer, M.A. Lynn, Inorg. Chim. Acta 243 (1996) 283.
[61] D.M. Baird, F.L. Yang, D.J. Kavanaugh, G. Finness, K.R. Dunbar, Polyhedron 15 (1996) 2597.
[62] A.B.P. Lever, Inorg. Chem. 29 (1990) 1271.
[63] A.B.P. Lever, in: A.J.L. Pombeiro, J.A. McCleverty (Eds.), Molecular ELectrochemistry of Inorganic, Bioinorganic and Organometallic Compounds, Kluwer Academic, Dordrecht, 1993.
[64] T.A. Budzichowski, M.H. Chisholm, K. Folting, Chem. Eur. J. 2 (1996) 110.